Behavioural Brain Research 432 (2022) 113968

Contents lists available at ScienceDirect

Behavioural Brain Research

journal homepage: www.elsevier.com/locate/bbr

Temporal, spatial and molecular pattern of dopaminergic neurodegeneration in the AAV-A53T α-synuclein rat model of Parkinson's disease

Thomas Musacchio [a], Jing Yin [a], Fabian Kremer [a], James B. Koprich [b,c], Jonathan M. Brotchie [b,c], Jens Volkmann [a], Chi Wang Ip [a,*]

[a] Department of Neurology, University Hospital of Würzburg, Department of Neurology, Josef-Schneider-Strasse 11, 97080 Würzburg, Germany
[b] The Krembil Research Institute, Toronto Western Hospital, University Health Network, 60 Leonard Avenue, 8KD402, Toronto, Ontario M5T 2S8, Canada
[c] Atuka Inc., First Canadian Place, 100 King Street West, Toronto, Ontario M5X 1C9, Canada

ARTICLE INFO

Keywords:
Parkinson's disease
α-synuclein
A53T
Neurodegeneration
HDAC1
Nrf2

ABSTRACT

Degeneration of the nigrostriatal tract is a neuropathological hallmark of Parkinson's disease (PD). A differential intraneuronal vulnerability of dopaminergic neurons within the substantia nigra (SN) has been suggested, starting as an axonopathy followed by neuronal cell loss that is accompanied with motor deficits. To date, there is no therapy available to delay or halt this neurodegeneration. Nuclear factor (erythroid-derived 2)-like-2 factor (Nrf2) and histone deacetylase 1 (HDAC1) are crucial molecular regulators that undergo nucleo-cytoplasmic shuttling and are involved in regulation of axonal and perikarya degeneration of neurons under various pathologic conditions. We here aimed to analyze the time course of dopaminergic neurodegeneration in an AAV PD rat model overexpressing human mutated A53T α-synuclein (haSyn), differentially correlate striatal terminal and SN perikarya loss with behavioral deficits and investigate if nucleo-cytoplasmic Nrf2 and HDAC1 expression are altered in dopaminergic perikarya of the haSyn PD rat model. We observed impaired motor performance in haSyn PD rats assessed by the single pellet reaching task at four- and six-weeks post AAV injection ($P < 0.05$ each). However, only striatal terminal loss correlated significantly with motor deficits in haSyn PD rats, indicating that parkinsonian motor features reflect the striatal dopaminergic denervation, but cannot be taken as an indirect measure of neurodegeneration per se. Immunofluorescence staining demonstrated an upregulation of HDAC1 in the dopaminergic cell nucleus ($P < 0.05$) while no changes were observed for Nrf2. These data suggest a critical functional role of the axonopathy on motor behavior in haSyn PD rats and mechanistically point towards an impaired nucleo-cytoplasmic translocation of HDAC1 and thus a potential role of disturbed histone acetylation in neurodegeneration.

1. Introduction

Parkinson's disease (PD) is the second most common neurodegenerative disorder after Alzheimer's disease [4]. Progressive degeneration of dopaminergic neurons in the substantia nigra (SN), dopaminergic axonal loss, denervation of terminals in the striatum and intracellular α-synuclein aggregates are the neuroanatomical correlates of the disease. As a result of degeneration affecting the nigrostriatal tract, basal ganglia motor networks become dysfunctional, with dominance of inhibitory outputs to the cortex resulting in motor symptoms such as bradykinesia and rigidity [16]. The mechanisms underlying neurodegeneration are poorly understood, and for the most common form of PD, sporadic (idiopathic) PD a causative factor can, by definition, not be identified. However, mutations in specific genes have been identified as causing non-sporadic PD. Amongst these, rare monogenetic mutations in the gene encoding for aSyn (SNCA) [29], offer a unique opportunity to study human molecular disease pathways in animal models of PD [35] particularly because mutated aSyn is considered to be directly linked to an early step in pathogenesis of the disease. Misfolding and insoluble aggregation of α-synuclein protein in neurons and their terminals (termed Lewy bodies and Lewy neurites, respectively) with concomitant cell death is undoubtedly the major neuropathologic

* Corresponding author.
E-mail address: ip_c@ukw.de (C.W. Ip).

https://doi.org/10.1016/j.bbr.2022.113968
Received 28 February 2022; Received in revised form 7 June 2022; Accepted 12 June 2022
Available online 20 June 2022

hallmark of the vast majority of PD, irrespective of etiology [34].

Interestingly, the nigrostriatal tract in PD presents differential intraneuronal vulnerability. A growing body of literature supports the notion that PD pathogenesis begins as an axonopathy followed by neuronal cell body degeneration conceptually framed as a dying back neuropathy [2,6,11,21,24,25]. Axonal damage in neurodegenerative disorders can arise from dysregulated nucleo-cytoplasmic shuttling of molecular regulators for neurodegeneration such as nuclear factor (erythroid-derived 2)-like-2 factor (Nrf2) that is described as a master regulator of oxidative stress and histone deacetylase 1 (HDAC1) demonstrates a role in epigenetic regulation [3,7,9,26,32]. The identification of these highly regulated molecular mechanisms of neurodegeneration led to numerous successful pre-clinical PD studies that prevented neuronal cell death. However, the common drawback of these preclinical studies was the use of toxin-mediated PD models, either by 1-methyl-4 phenyl 1,2,3,6-tetrahydropyridine (MPTP) [1,8,13,15] or 6-hydroxydopamine (6-OHDA) [37] that do not adequately reflect the molecular pathology of human PD and therefore have limited translational value for studying neuroprotective therapies. The PD model used in the current study is based on a vector driven (adeno-associated virus [AAV] 1/2) overexpression of human mutated A53T aSyn (haSyn) in dopaminergic SN neurons leading to progressive degeneration of the nigrostriatal tract, motor impairment and accumulation of pathologic Lewy-like structures thereby mimicking the neurobiological hallmarks of PD. Therefore, this model is better suited for the analysis of the mechanism of differential PD neurodegeneration [18,19,23].

In this study, we addressed time course and spatial development of neurodegeneration of dopaminergic neurons in different compartments of the nigrostriatal tract in the haSyn PD rat model and correlated different biomarkers of disease-related nigrostriatal neurodegeneration with motor impairment. Moreover, as preclinical data on the role of HDAC1 in PD is contradictory [3,10,17,33] and because genetic variants of Nrf2 are strongly associated with human PD [20,36], we aimed to analyze the mechanism of dopaminergic neurodegeneration in this model more in detail by investigating the spatial distribution of Nrf2 and HDAC1 that are involved in the regulation of axonal and cell soma degeneration in neurodegenerative diseases.

2. Methods

2.1. Animals

93 adult Sprague Dawley rats were purchased from Charles River Laboratories, Sulzfeld, Germany and kept under standard conditions (12 h light-dark cycle, 21 °C) with free water and food supply. To avoid possible hormonally induced bias regarding behavioral testing and the investigation of neurodegeneration only male animals were used. Surgical interventions were performed at an average weight of 280 g. All applicable international, national, and/or institutional guidelines for use and care of animals were followed (EU Directive 2010/63/EU for animal experiments). The local authorities at the government of Lower Franconia, Würzburg, Germany, approved all animal experiments (License Number: RUF 55.2.2-2532.2-767).

2.2. Behavioral tests

To minimize the variance inherent in all movement sequences with respect to the dominant brain hemisphere the handedness of the animals was determined before the injection of the viral vector with subsequent injection to the contralateral SN. Due to the intended lateralized motor phenotype appropriate tests for the investigation of lateral differences or use of the dominant forepaw, which have proven there reliability even for assessment in this animal model, were selected.

2.2.1. Single pellet reaching task

Under standardized conditions (always at the same time point during the morning), animals were placed in a Plexiglas box (34 x 14 cm) with an opening on the side filled with a food pellet and trained to grasp and pass the pellet to their mouth as described [23]. The sessions were videorecorded, and the first 20 reaching attempts were scored per session. For scoring, the investigator was blinded to experimental groups. A score of 1 equaled a successful grasp attempt with immediate delivery of the pellet to the animal's mouth, scoring of 0.5 was given when the pellet dropped to the ground before eating and a score of 0 corresponded to a failed attempt. The first three days of training were used to assess handedness of the rats which were then trained to grasp with their dominant hand 10 min per day for 19 days prior the injection of the AAV. Motor performance was assessed with the investigator blinded to treatment conditions at the time points preoperative/baseline and two, four and six weeks after injection. Values were calculated relative to pre-operative baseline analyzes. Training sessions were performed every 5 days, in between assessments, but not scored. Two animals were excluded from the study because of insufficient performance at baseline.

2.2.2. Cylinder test

The cylinder test was used to assess spontaneous forepaw use at baseline before injection of the vector and 2, 4 and 6 weeks afterwards. Rats were placed into a transparent plexiglass cylinder of 20 cm diameter and 30 cm height in front of two mirrors and were video recorded for a duration of 10 min. The videos were scored post-hoc by an observer blinded to the treatment condition. Each rearing of the rat was analyzed for the number of touches of the inner surface of the cylinder with either the ipsilateral (regarding the side of vector injection), contralateral or both forepaws simultaneously. Final data is presented as percentage of the ipsilateral forepaw use by calculation with the equation: [(ipsilateral paw + 0.5 both paws) / (ipsilateral paw + contralateral paw + both paws)] x 100. A minimum of 20 total touches was considered acceptable for inclusion in the analysis.

2.3. Adeno associated vector (AAV) 1/2 serotype injection

Stereotactic surgeries were performed as described [19,23]. In brief, injections were made unilaterally into the SN contralateral to the dominant forepaw with either 2.0 μl of empty AAV1/2 (empty vector; EV, n = 33) or 2.0 μl AAV1/2 expressing human mutated haSyn both at a concentration of 2.55×10^{12} genomic particles (gp)/ml (n = 36) by using following coordinates from Bregma: − 5.1 mm AP; either − 2.0 mm (right) or + 2.0 mm (left) ml; − 7.4 mm DV according to the rat brain atlas of Paxinos and Watson [27]. Vectors were purchased from Genedetect®, Basel, Switzerland.

2.4. Experimental sequence

19 days before stereotactic AAV1/2 injection, all animals were trained for the single pellet reaching task and baseline motor performance was assessed just before injection. The vector injection took place at day 0 (baseline) and it resulted an empty vector (EV) and an AAV1/2-A53T-aSyn parkinsonian rat group. On day 14 (week 2), 28 (week 4) and 42 (week 6) behavioral testing and necropsy for tissue processing and further analysis took place.

2.5. Tissue processing

2.5.1. Horizontal 10° fresh frozen sections

Rats were transcardially perfused with 0.1 M phosphate buffered saline (PBS) and the brains were carefully extracted in total. After washing with PBS brains were placed horizontally with the basal part on a cryomold filled up with Tissue-Tek® O.C.T. and snap-frozen in dry ice cooled methylbutane. Afterwards the brains were horizontally cryosectioned with a + 10° angle into 10 μm sections for immunohistochemistry of the nigrostriatal tract.

2.5.2. Coronal free-floating sections

Brains were dissected coronally at the region of − 0.26 mm from Bregma. The dorsal part including the SN was immersion-fixed in 4 % paraformaldehyde (PFA) in 0.1 M PBS for two days and afterwards cryo-protected in 30 % sucrose/0.1 M PBS solution for another four days followed by freezing in Tissue-Tek® O.C.T. 40 μm coronal cryo-sections of the brain at the region − 4.36 to − 6.72 mm relative to Bregma covering the whole SN were serially cut (six series).

2.6. Immunohistochemistry

2.6.1. Tyrosine hydroxylase (TH)/Nissl staining

TH staining was used to visualize the dopaminergic nigrostriatal tract in the horizontal 10° sections and for labeling dopaminergic neurons in the SN of the 40 μm coronal sections. After post-fixation with 4 % PFA for 15 min tissue was blocked for 1 h at room temperature (RT) with 2 % normal bovine serum (BSA) and 10 % normal goat serum (NGS) in 0.1 M PBS and then incubated overnight with rabbit anti-rat TH primary antibody (Abcam, Cambridge, UK) diluted in 2 % BSA and 2 % NGS in 0.1 M PBS. A biotinylated secondary goat-anti-rabbit-antibody was applied for 2 h at RT, followed by avidin/biotin reagent (Dako, High Wycombe, UK) before incubation and staining with diaminobenzidine-HCl (DAB) and H_2O_2 (Vector Labs, Burlingame, USA). After TH staining coronal 40 μm sections were then incubated in cresyl violet solution (1 g cresyl violet + 10 ml 100 % acetic acid ad 1 l distilled water) for 30 min at RT for Nissl staining. After washing in distilled water, sections were dehydrated in an ascending series of ethanol (70 %, 96 %, 100 %) and then incubated in xylene solution (St. Louis, Missouri, USA).

2.6.2. TH/aSyn Immunofluorescence double staining

After post-fixation with 4 % PFA for 15 min sections were blocked with 5 % NGS and 5 % BSA in 0.1 M PBS for 1 h at RT and simultaneously incubated overnight at 4 °C with primary chicken-anti-rat TH (Abcam, Cambridge, UK) and mouse anti-human aSyn (Invitrogen, Maryland, USA) antibodies followed by incubation with fluorescence labeled goat-anti-chicken Cy3 (Alpha Diagnostics cat # 60334, San Antonio, Tx, USA) and goat-anti-mouse Cy2 (Jackson ImmnoResearch Laboratories Inc., West Grova, PA) secondary antibodies for 1 h at RT. DAPI nuclear staining (Sigma Aldrich, Missouri, USA) was performed at RT for 20 min

2.6.3. TH/Nrf2 and TH/HDAC1 immunofluorescence double staining

For double-immunofluorescence stainings of TH and either Nrf2 or HDAC1 all protocol steps, solutions and the antibodies for TH staining as described above remained unchanged. For Nrf2 the primary antibodies rabbit-anti-rat Nrf2 (GeneTex, USA) and for HDAC1 rabbit-anti-rat HDAC1 (Thermo Fischer, USA) were used. The secondary antibody used for both was goat-anti-rabbit alexa fluor 488 (Invitrogen, USA). An additional DAPI nuclei staining was then performed.

2.7. Unbiased stereology and relative cell count of SN neurons

Stereology was performed with the StereoInvestigator software package (version 11.07; MicroBrightField Biosciences, Williston, VT). The investigator was blinded for experimental groups. Twelve coronal SN sections in average separated by 240 μm (1/6 series) were used for counting. TH^+ or $Nissl^+$ neurons in both SN pars compacta and reticulata were included for quantification. Counting parameters were: grid size 130 × 130 μm, counting frame 60 × 60 μm and 1.5 μm guard zone. Actual mounted thickness was determined by randomly selecting sections and determining thickness at every counting site. Sections were viewed under a 100 x/1.25 numerical aperture objective (Olympus) on a BX53 microscope. Gundersen coefficient of error for m= 1 were all less than or equal to 0.09 for each section counted. On DAB-stained 10° horizontal sections of the nigrostriatal tract cell bodies in the SN were counted manually using four sections per animal and a 10x objective. Relative cell count was calculated by dividing the absolute numbers of injected to the uninjected side.

2.8. Image processing

2.8.1. Optical density of dopaminergic fibers in striatum

TH optical density of the dopaminergic TH^+ fibers in striatum was analyzed on the horizontal 10°, DAB-stained sections by using ImageJ software (NIH) after brightfield pictures were taken using identical exposure times and settings. Original images were transformed into 8-bit greyscale images. Relative optical density was calculated by dividing the density values of the injected by the uninjected side after subtracting the signal of the non-specifically stained background of the corpus callosum.

2.8.2. Immunofluorescence intensity of Nrf2 and HDAC1 in the SN

Immunofluorescence images from the SN of either Nrf2 or HDAC1 combined with TH were transformed into 16-bit greyscale images using ImageJ and then black and white inverted to enhance the contrast of the stained structures to mark the region of interest (ROI). For the analysis of differential nucleus-cytoplasmic distribution, immunofluorescence intensity of nuclei and cytoplasm of ten dopaminergic SN perikarya on two sections for each animal were investigated separately using a 100x objective. Within the perikarya, nuclei were identified by DAPI staining. Borders of nuclei and cytoplasm (borders from Nrf2 or HDAC1 signal respectively) were manually drawn and measured separately for the immunofluorescence intensity. Additionally, the background was measured for each position in the proximity of selected ROI in the extracellular tissue. Nucleo-cytoplasmic immunofluorescence intensity ratio was calculated by subtracting the non-specifically stained background signal from both the nucleus and the cytoplasm and by then dividing the corrected intensity values of the nucleus by the values of the cytoplasm.

2.9. Statistical analysis

Statistical analysis was performed using Graphpad Prism 9 software (Graphpad Software, San Diego, USA). Normal distribution was tested by using Shapiro Wilk normality test. For the single pellet reaching task, analysis of TH^+ optical density in striatum, stereological estimation of cell counts in the SN the parametric one-way analysis of variance (ANOVA) test with Tukey's multiple comparison post-test was performed. For immunofluorescence intensity analysis of Nrf2 and HDAC1 in the SN comparing EV with haSyn PD rats, the parametric students t-test was implemented. Correlations were calculated using Pearson r followed by a subsequent linear regression analysis. *$p < 0.05$, * *$p < 0.01$ and * **$p < 0.001$ were considered as significant p-values.

3. Results

3.1. Confirmation of haSyn expression in the SN of haSyn PD rats

To verify expression of human mutated A53T aSyn in the SN of haSyn PD rats, immunofluorescence double staining for TH/aSyn was performed. Six haSyn PD rats were excluded from the study because there was no detectable signal of aSyn staining after injection of the haSyn vector. As expected, in EV injected animals, no haSyn expression could be observed in the SN nor in the uninjected side of haSyn PD rats used as an additional control (Fig. 1).

3.2. Progressive motor deficits in haSyn PD rats

Motor skill in rats was assessed by the success rate in the single pellet reaching task and the paw use in cylinder test relative to the pre-OP (baseline) performance. Two weeks after AAV1/2 injection, no obvious motor deficit was found in haSyn PD rats compared to controls. Over time, a significant decrease of the relative success in the single pellet reaching task was observed in haSyn PD rats (time point 2w:

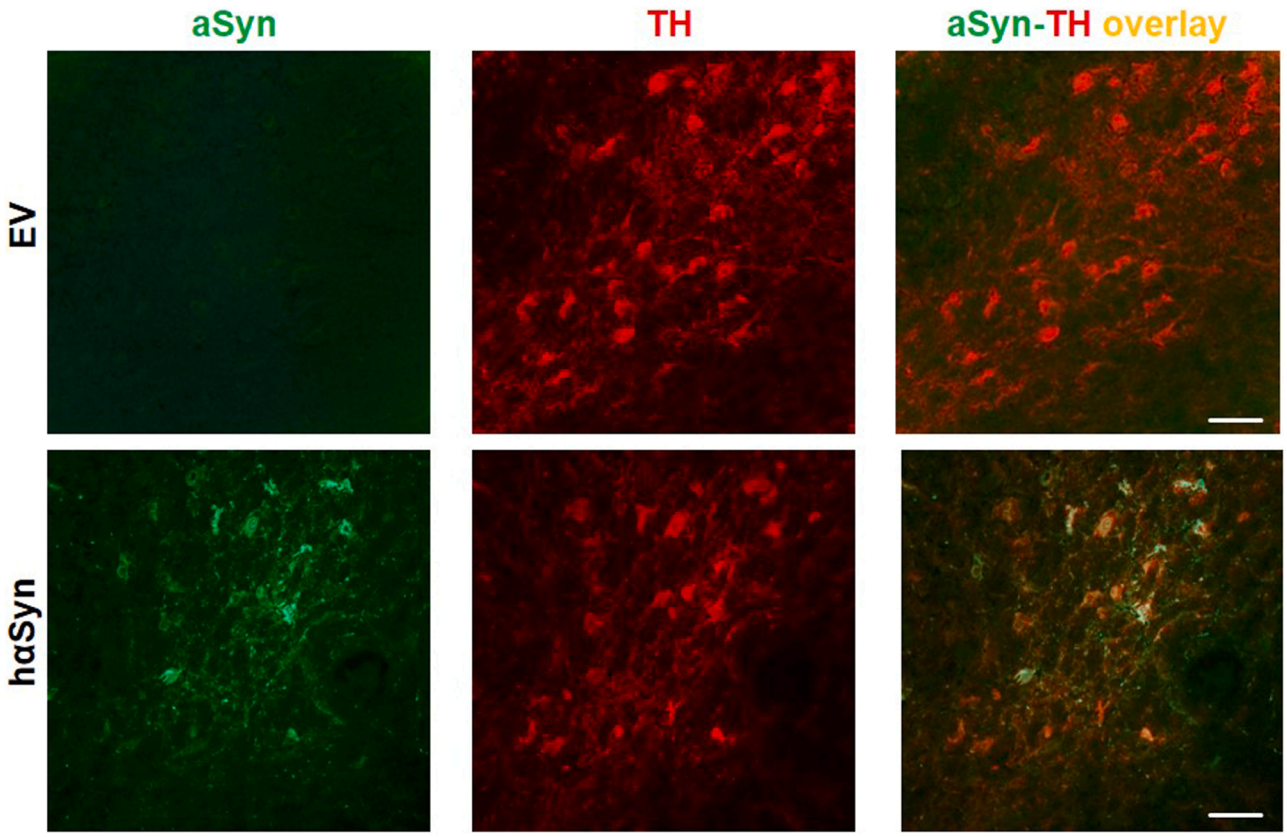

Fig. 1. : Expression of α-synuclein in the substantia nigra of AAV-injected haSyn PD rats. Representative immunofluorescence stainings for α-synuclein (aSyn, green) and tyrosine hydroxylase (TH^+) positive dopaminergic neurons (red) in the substantia nigra of empty vector (EV) and human mutated A53T-aSyn vector (haSyn) injected animals. Scale bar: 50 μm each. (For interpretation of the references to color in this figure legend, the reader is referred to the web version of this article.)

78.35 ± 16.91, 4w: 36.51 ± 8.27, 6w: 28.33 ± 6.46; mean ± standard error of the mean [SEM]) compared to the respective EV controls (time point 2w: 95.56 % ± 8.55, 4w: 94.61 ± 9.23, 6w: 101.7 ± 12.79), four and six weeks after AAV delivery (Fig. 2A). Even more pronounced changes in the paw use of haSyn PD rats with preference for the ipsilateral paw could be observed over time in the cylinder test (EV 2w:

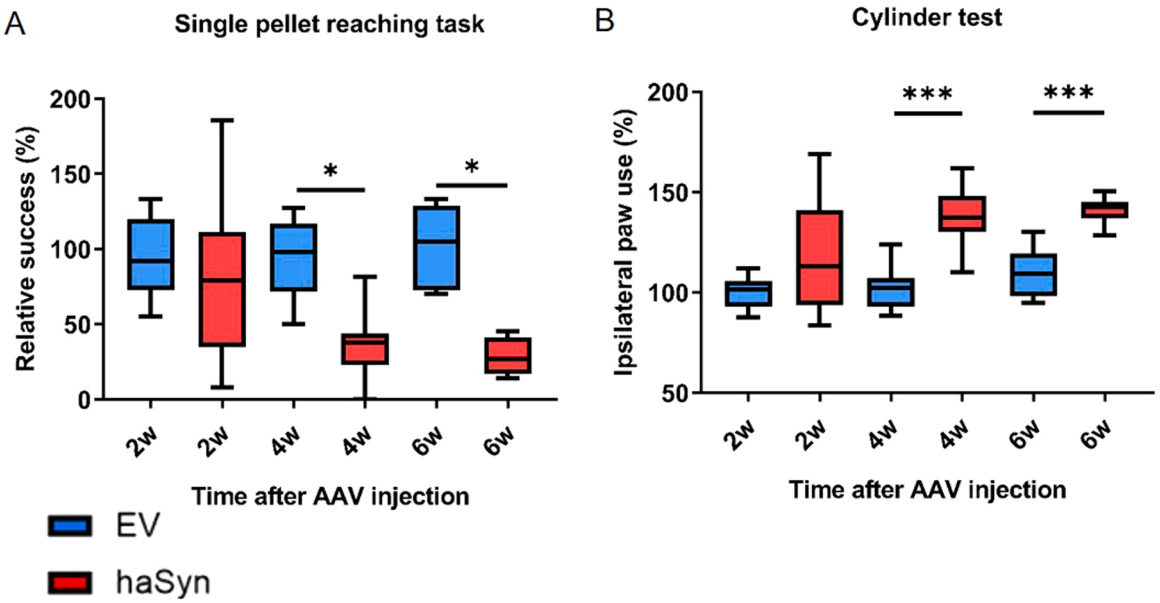

Fig. 2. : Progression of motor deficits over time in haSyn PD rats. A, B Group comparison of relative success in single pellet reaching task (A) and forepaw use in cylinder test (B) in EV (blue) and haSyn rats (red) at two, four and six weeks after AAV delivery to evaluate progression of motor deficits over time. Statistical analysis was performed using one-way ANOVA followed by Tukey's multiple comparison test (n = 4–11): Pellet reaching: $F(5, 39) = 5.499$, $P = 0.0006$; Cylinder Test: $F(5,52) = 4.784$, $P = 0.0011$. *$p < 0.05$, $p < 0.001$ *** . All data are shown as box and whisker plots + min/max. (For interpretation of the references to color in this figure legend, the reader is referred to the web version of this article.)

99.81 ± 2.22, haSyn 2w: 117.3 ± 8.32, EV 4w: 102.3 ± 3.96, haSyn 4w: 137.7 ± 5.39, EV 6w: 109.5 ± 3.79, haSyn 6w: 141.2 ± 6.46) at four and six weeks time points (Fig. 2B).

3.3. Progressive degeneration of the nigrostriatal tract in haSyn PD rats

Over the observation period of six weeks, there was progressive reduction of TH^+ dopaminergic SN neurons and total $Nissl^+$ SN neuron number in haSyn PD rats. In contrast, unbiased stereology demonstrated stable neuronal counts in EV controls. The estimated cell number of dopaminergic SN neurons was significantly reduced in haSyn rats four weeks after AAV1/2 injection and even more pronounced at six weeks time point (Fig. 3A,C) (EV 2w: 11129 ± 624, haSyn 2w: 8075 ± 486, EV 4w: 11308 ± 541, haSyn 4w: 7402 ± 934, EV 6w: 10912 ± 640, haSyn 6w: 5114 ± 1177). Interestingly, although a progressive decline of $Nissl^+$ total neuron number within the SN was observed across the period of evaluation, only the six-week time point yielded a statistically significant reduction of cell number in haSyn PD rats (Fig. 3D) (EV 2w: 31460 ± 1358, haSyn 2w: 28113 ± 916, EV 4w: 29949 ± 786, haSyn 4w: 23291 ± 2625, EV 6w: 30701 ± 852, haSyn 6w: 22345 ± 3130). Analysis of dopaminergic projections to the striatum showed a progressive decrease in optical density of TH^+ fibers within the striatum in haSyn PD rats. The relative optical density of TH^+ fibers within the striatum was significantly decreased, comparing haSyn PD to EV rats, at six weeks' time point (Fig. 3B,E) (EV 2w: 1.167 ± 0.140, haSyn 2w: 0.903 ± 0.035, EV 4w: 1.001 ± 0.033, haSyn 4w: 0.787 ± 0.039, EV 6w: 1.008 ± 0.046, haSyn 6w: 0.597 ± 0.047). This reduction was also significant when comparing the six weeks haSyn PD group to the two weeks and four weeks EV rats (Fig. 3B,E).

3.4. Progressive motor deficits correlate with striatal dopaminergic denervation but not with dopaminergic perikarya loss

To determine whether reduction of dopaminergic perikarya number in the SN or rather loss of dopaminergic terminals in the striatum are relevant for the motor symptoms in haSyn PD rats at six weeks' time point, we performed correlation analyses with subsequent linear regression. Because of differential tissue processing to be able to correlate molecular degeneration markers with dopaminergic degeneration, unbiased stereology data for this subgroup of animals were not available. However, to obtain most comparable results, we analyzed dopaminergic neurons and striatal fibers in the same sections for each animal by using a novel brain sectioning method to generate horizontal slides with a 10° angle (Fig. S1). Using these sections, we quantified the dopaminergic neurons in the area of the injected SN relative to the non-injected contralateral SN for the estimation of neuron loss as described previously [12]. Although the linear slope ($r = -0.61$) shows a clear downward trend, motor deficits assessed by the single pellet reaching task did not correlate significantly with the loss of dopaminergic perikarya in the SN (Fig. 4A). In contrast, a significant correlation was found between the relative success in pellet reaching task and the striatal optical density of dopaminergic terminals ($p < 0.05$, $r = -0.73$) (Fig. 4B). A similar, yet more pronounced result could be obtained when correlating cylinder test data with dopaminergic denervation in the striatum ($p < 0.05$, $r = 0.78$) (Fig. 4D) while correlation to perikarya loss remained unsignificant ($r = 0.32$) (Fig. 4C). Furthermore, no significant correlation could be found between TH perikarya and fiber loss ($r = 0.45$, $p = 0.20$) therefore indicating that these two groups can be considered separately for the above mentioned analysis.

3.5. Alteration of differential nucleo-cytoplasmic distribution of HDAC1 but not Nrf2 in dopaminergic cell soma of haSyn PD rats

For a deeper mechanistic insight into dopaminergic neurodegeneration, we analyzed molecular regulators of neuronal degeneration, which are known to undergoe nucleo-cytoplasmic shuttling. For this, the immunofluorescence intensity of Nrf2 and HDAC1 were analyzed in the dopaminergic SN perikarya at six weeks time point after AAV delivery (Fig. 5). For Nrf2 no significant changes were found comparing the nucleo-cytoplasmic ratio of haSyn PD rats with controls (Fig. 5A,C). In contrast, HDAC1 immunofluorescence intensity in dopaminergic cell soma of haSyn PD rats demonstrated a shift to the nuclei, thereby resulting in a significantly elevated nucleo-cytoplasmic ratio compared to EV control (Fig. 5B,D).

4. Discussion

Previous studies have supported the pathogenetic concept that dopaminergic axonal degeneration of the nigrostriatal tract precedes cell soma degeneration in PD. With attention to temporal pattern and subcellular compartmental distribution of dopaminergic neurodegeneration we found a significant loss of dopaminergic SN perikarya and terminals in the pathophysiologically relevant haSyn PD rat model as early as four weeks after viral vector injection. Underlining the chronic progressive nature of this model, severity of dopaminergic damage in the nigrostriatal tract during our investigation time period reached the maximum at six weeks' time point after AAV1/2 delivery. However, only loss of the most distantly located terminals and not of cell soma correlated significantly with motor deficits in haSyn PD rats. This finding could explain variance and magnitude of the observed motor phenotype better than cell soma degeneration alone thereby emphasizing the functional role of the axonopathy in this PD model. In line with this observation, estimation of dopaminergic neuron and striatal axon/terminal loss in PD patients suggested that at the time of motor symptom onset the degree of axonal and terminal loss exceeds the loss of dopaminergic cell bodies in the SN [2] indicative for a more pronounced vulnerability of axons and terminals compared to perikarya in PD. With focus on axons, a compartmental analysis of pathological aSyn aggregates in peripheral autonomic neurons of PD patients showed that pathology was predominantly at the distal axonal region in contrast to the low aSyn level observed in the sympathetic ganglia as a sign for centripetal degeneration of the cardiac sympathetic nerves [25]. The occurrence of dopaminergic terminal and axon loss before degeneration of perikarya was already demonstrated using the same haSyn viral vector but at a lower titer of 1.76×10^{12} gp/ml. This less severe haSyn PD model showed a significantly reduced expression of dopaminergic terminals in the striatum three weeks after intra-nigral injection of A53T-aSyn encoding AAV1/2, while at the same time point, no loss of dopaminergic SN cell number was observed [18]. The predominance of axonal damage in preclinical PD models is not confined to the haSyn PD models but was also observed in the MPTP macaque model of PD that demonstrated a marked reduction of dopaminergic axons prior to the loss of SN cell bodies [11,21].

We evaluated molecular regulators of neurodegeneration, in particular those proteins associated with aSyn (dys)function or PD and described to be controlled by nucleo-cytoplasmatic shuttling such as Nrf2 and HDAC1 [3,7,9,26,32]. Histone acetylation is an important epigenetic mechanism controlling for gene expression. This process is tightly regulated by histone acetyl transferases (HATs) and HDACs. Dysregulated acetylation of histone proteins has been proposed to play a role in the pathophysiology of neurodegenerative diseases. As such, histone hypoacetylation is described in experimental models of neurodegenerative diseases such as in Huntington's disease [31]. Treatment of the MPTP mouse model of PD with a specific HDAC1 and 2 inhibitor prevented loss of dopaminergic neurons in the SN, thereby underlining the neurodegenerative role of histone hypoacetylation [3]. In line with this finding, studies in LRRK2 transgenic mice [17] as well as in the toxic lactacystin model of PD [10] using valproate, which acts as an HDAC-inhibitor, showed a neuroprotective effect and a restoration of motor functions. However, neurodegeneration does not exclusively take place by histone hypoacetylation, but increased acetylation of histone proteins has also been found to promote degeneration of dopaminergic

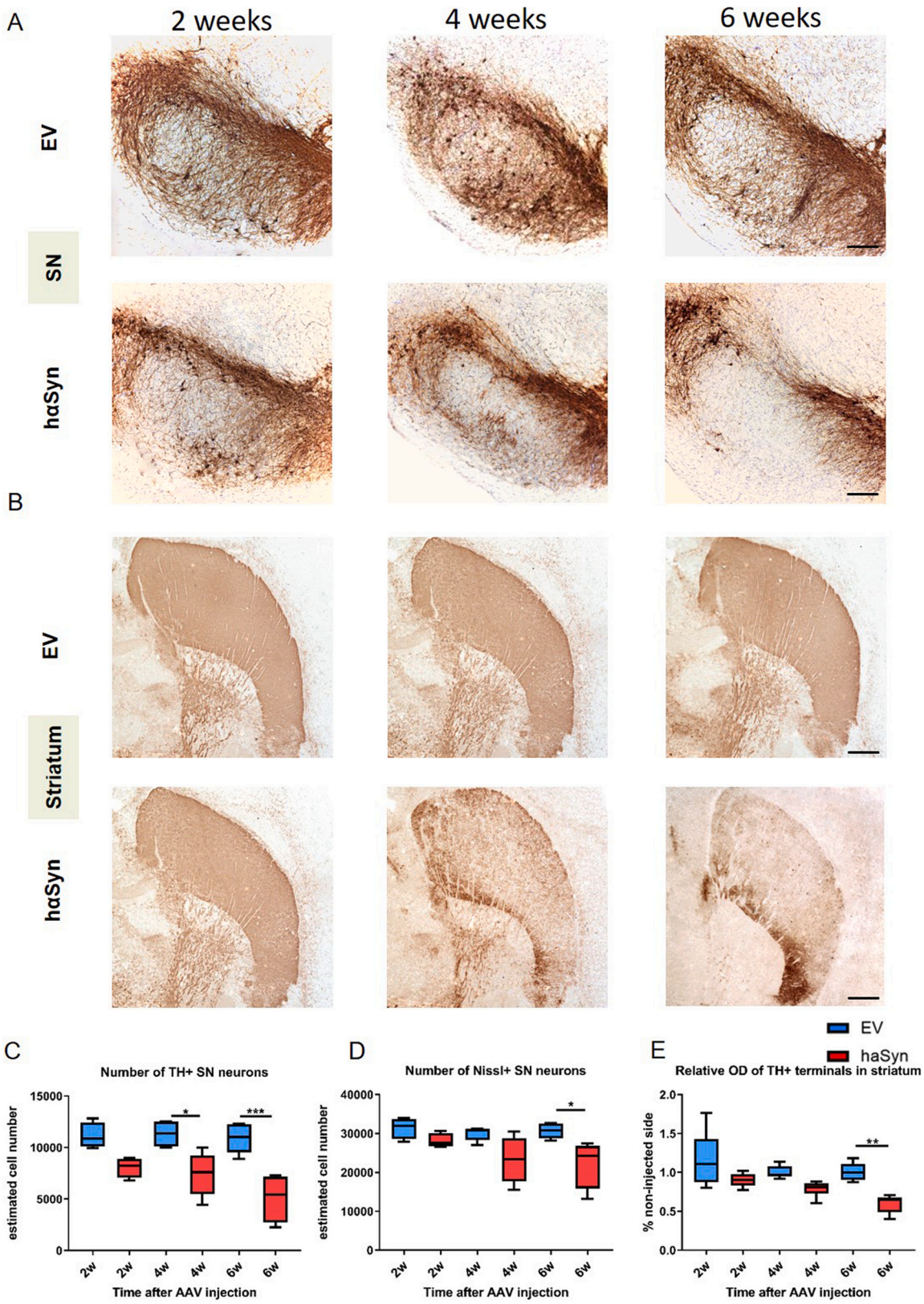

Fig. 3. : Progressive degeneration of the dopaminergic nigrostriatal tract in haSyn PD rats. A-E, Immunohistochemical staining of TH^+ dopaminergic neurons in the substantia nigra (A) and the corresponding dopaminergic fibers/striatal terminals (B) at two, four and six weeks after AAV injection demonstrates progressive degeneration in the haSyn group corresponding to a reduced estimated cell number of TH^+ SN neurons (C), number of total $Nissl^+$ neurons (D), and relative optical density measurement of TH+ terminals in the striatum (E). Statistical analysis was performed using one-way ANOVA followed by Tukey's multiple comparison test (n = 4–6): TH^+ neurons: $F(5, 21)= 10.52$, $P < 0.0001$); $Nissl^+$ neurons: ANOVA results: $F(5, 21)= 4.534$, $P = 0.0058$; TH^+ terminals: $F(5, 30)= 8.394$, $P < 0.0001$); All data are shown as box and whisker plots + min/max. *p < 0.05, **p < 0.01. Scale bar: 200 μm each.

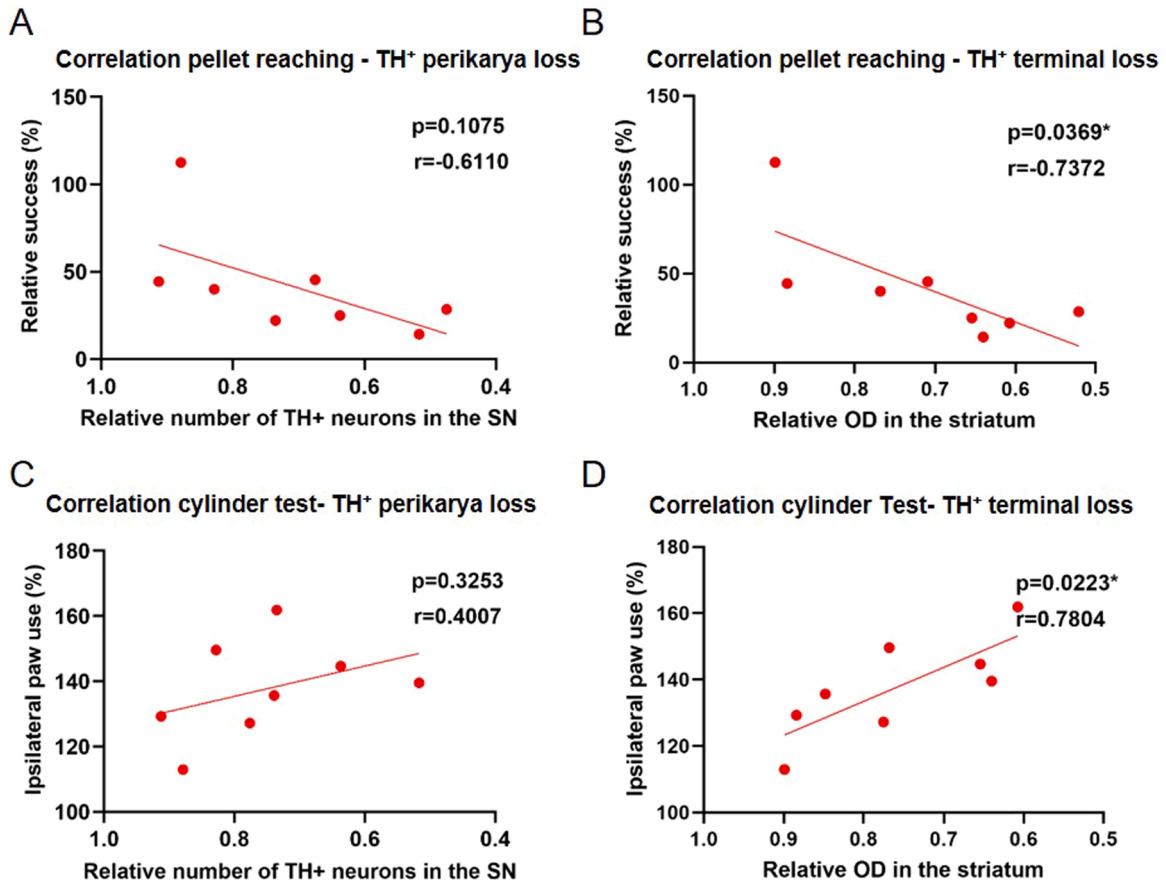

Fig. 4. : Motor deficits in haSyn PD rats correlate with dopaminergic terminal loss in the striatum. A-D, Decline of motor performance in relative single pellet reaching task (A,B) and forepaw use in cylinder test (C,D) does not correlate to the relative number of TH^+ neurons in the substantia nigra (A,C) but correlates significantly to the loss of dopaminergic terminals in the striatum (B,D) using simple linear regression analysis. A $r = -0.6110$, $p = 0.1075$, B $r = -0.7372$, $p = 0.0369$ *, C $r = 0.4007$, $p = 0.3253$, D $r = 0.7804$, $p = 0.0223$ *.

midbrain neuronal cells after exposure to neurotoxic pesticides [33]. Because of these discrepant findings, we aimed to assess the subcelluar distribution and expression levels of HDAC1 in the nigrostriatal tract of the haSyn PD model. We observed a significantly elevated nucleo-cytoplasmic ratio of HDAC1 expression in the remaining dopaminergic SN perikarya of haSyn PD rats during late disease stage of six weeks, thereby pointing towards a reduced translocation of HDAC1 from the nucleus to the cytoplasm. We suggest that histone hypoacetylation due to elevated HDAC1 expression in surviving dopaminergic neurons promotes neuroprotection. In keeping with this finding, a neuroprotective role of HDAC1 by interacting with histone deacetylase-related protein and thereby preventing c-Jun phosphorylation and expression has been reported [22]. In addition, stimulation of HDAC1 activity by sirtuin 1, a NAD^+-dependent deacetylase, was shown to protect neurons by repairing DNA double-strand breaks [5]. Our data thereby suggests a possible neuroprotective role of HDAC1 in haSyn PD rats. Further studies in this model, such as implementation of HDAC1 inhibitors, would be useful to assess the role of HDAC1 translocation to the nucleus on target gene expression levels and downstream protein (dys-)regulations to gain more insights on the mechanisms of possible neuroprotection.

Nrf2 is a nuclear transcription factor for genes involved in antioxidative defense and therefore acts neuroprotective if translocated from the cytoplasm to the nucleus under pathological conditions [7,14]. It is therefore considered antidegenerative or even neuroprotective in function. Elevated expression levels of Nrf2 in the nucleus of nigral cells of human PD patient autopsies compared to non-PD controls were described, and a possible delay of degeneration in surviving nigral neurons mediated by Nrf2 has been suggested [30]. Further studies revealed a cell-autonomous aSyn detoxicating mechanism of Nrf2 with the ability to increase aSyn degradation and therefore reduce toxicity investigated at single cell level [32]. A recent study even demonstrated a systemic activation of the Nrf2 pathway in PD patients found in blood leukocytes thereby emphasizing the role of Nrf2 in PD pathogenesis [28]. In haSyn PD rats we did not find any significant changes in the differential expression of Nrf2 within the SN cell soma by separately analyzing nuclei and cytoplasm. This finding is in contrast to the proposed translocation of Nrf2 from the cytoplasm to the nucleus during a pathological condition. This points to the potentially impaired ability of SN neurons to express antioxidative signals. We therefore assume that Nrf2 is not a key player in degeneration of dopaminergic neurons in the haSyn PD model, at least not in the here described stage of disease.

In summary, we here demonstrate hints that the emerging motor deficits in haSyn PD rats could be consequences of the nigrostriatal dopaminergic degeneration correlating to the degree of striatal terminal loss in a time-dependent manner. The shift of HDAC1 towards the nuclei could reflect a pathognomonic pattern of haSyn-dependent parkinsonian neurodegeneration in this model. However, these findings do not allow for conclusions about the molecular interactions of the investigated proteins with aSyn or other protein-protein interactions. Another limitation of the study is, that with the here presented experimental design and time course of disease it is not possible to distinguish between prodromal and motor manifest PD stages. Moreover, there are no conclusions possible on non-motor symptoms. Nonetheless, our results give new insights on the onset of motor dysfunction as well as on protein alterations of dopaminergic neurons in the haSyn PD rat model.

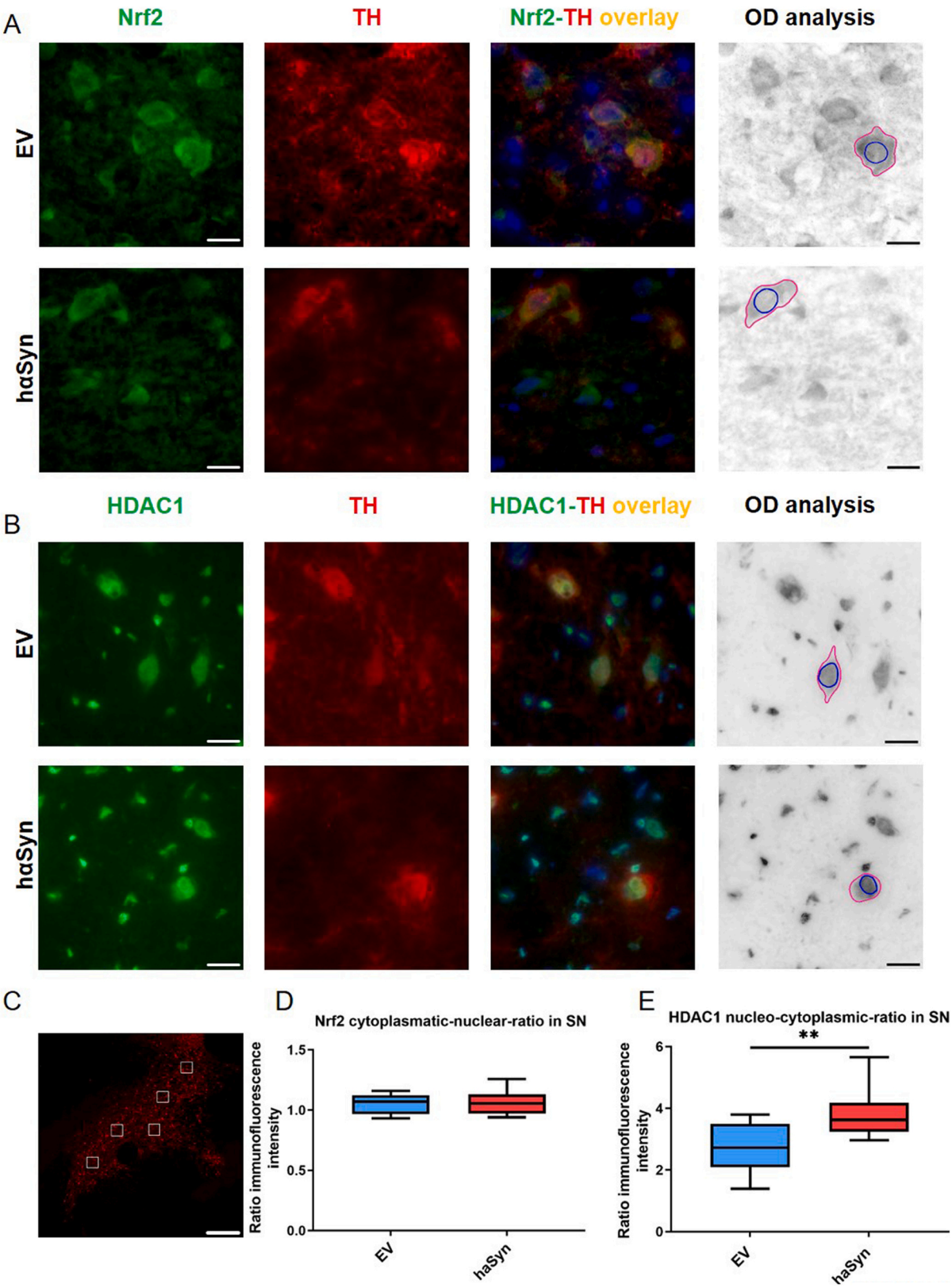

Fig. 5. : Differential distribution analysis of Nrf2 and HDAC1 in the SN of haSyn PD and control rats. A-B, Double immunofluorescence staining of either Nrf2 (A) or HDAC1 (B) (green), TH (red) and corresponding overlay images of the substantia nigra at six weeks' time point after AAV injection of both EV and haSyn groups, as well as greyscale pictures depicting the cellular and nuclear borders of Nrf2 (A, pink), HDAC1 (B, pink) and DAPI (blue) signal respectively C TH immunofluorescence staining of the substantia nigra in 10x objective indicating the regions of interest (white boxes) for immunofluorescence intensity measurement of Nrf2 or HDAC1 signal at higher magnification. D,E, Analysis of differential nucleus/cytoplasm distribution of immunofluorescence intensity for Nrf2 (D) and HDAC1 (E). Statistical analysis was performed by two-tailed t-test (n = 8–12): HDAC1: $t(18) = 2.976$, $p = 0.0081$. Data are shown as box and whisker plots + min/max. **$p < 0.01$. Scale bar: 15 μm (A,B,C) each, 200 μm (C). (For interpretation of the references to color in this figure legend, the reader is referred to the web version of this article.)

Moreover, they allow to better model and interpret biomarkers and symptom evolution of human PD, in particular when testing disease modifying strategies.

CRediT authorship contribution statement

Thomas Musacchio: Writing – original draft, Formal analysis, Investigation, Visualization. **Jing Yin:** Visualization, Formal analysis. **Fabian Kremer:** Visualization, Formal analysis. **James B. Koprich:** Writing – review & editing. **Jonathan M. Brotchie:** Writing – review & editing. **Jens Volkmann:** Writing – review & editing. **Chi Wang Ip:** Conceptualization, Funding acquisition, Supervision, Validation, Writing – original draft, Writing – review & editing.

Conflicts of Interest

Nothing to report.

Acknowledgements

This work was funded by the Deutsche Forschungsgemeinschaft (DFG, German Research Foundation) Project-ID 424778381-TRR 295 (A01 to J.V., A06 to C.W.I.), by the Interdisciplinary Center for Clinical Research (IZKF) at the University of Würzburg and by the Nündel Stiftung. J.Y. was funded by the China Scholarship Council. We thank Veronika Senger, Heike Menzel and Louisa Frieß for their technical assistance.

Author's contribution

C.W.I. concepted the study and designed the experiments. T.M., J.Y., F.K. acquired and analyzed data. C.W.I., T.M. wrote the manuscript. J.M. B., J.B.K., J.V. reviewed the manuscript.

Appendix A. Supporting information

Supplementary data associated with this article can be found in the online version at doi:10.1016/j.bbr.2022.113968.

References

[1] M. Ahuja, N. Ammal Kaidery, L. Yang, N. Calingasan, N. Smirnova, A. Gaisin, I. N. Gaisina, I. Gazaryan, D.M. Hushpulian, I. Kaddour-Djebbar, W.B. Bollag, J. C. Morgan, R.R. Ratan, A.A. Starkov, M.F. Beal, B. Thomas, Distinct Nrf2 signaling mechanisms of fumaric acid esters and their role in neuroprotection against 1-Methyl-4-Phenyl-1,2,3,6-tetrahydropyridine-induced experimental Parkinson's-like disease, J. Neurosci. 36 (2016) 6332–6351.
[2] H.C. Cheng, C.M. Ulane, R.E. Burke, Clinical progression in Parkinson disease and the neurobiology of axons, Ann. Neurol. 67 (2010) 715–725.
[3] C.J. Choong, T. Sasaki, H. Hayakawa, T. Yasuda, K. Baba, Y. Hirata, S. Uesato, H. Mochizuki, A novel histone deacetylase 1 and 2 isoform-specific inhibitor alleviates experimental Parkinson's disease, Neurobiol. Aging 37 (2016) 103–116.
[4] L.M. de Lau, M.M. Breteler, Epidemiology of Parkinson's disease, Lancet Neurol. 5 (2006) 525–535.
[5] M.M. Dobbin, R. Madabhushi, L. Pan, Y. Chen, D. Kim, J. Gao, B. Ahanonu, P. C. Pao, Y. Qiu, Y. Zhao, L.H. Tsai, SIRT1 collaborates with ATM and HDAC1 to maintain genomic stability in neurons, Nat. Neurosci. 16 (2013) 1008–1015.
[6] K. Doppler, H.M. Jentschke, L. Schulmeyer, D. Vadasz, A. Janzen, M. Luster, H. Hoffken, G. Mayer, J. Brumberg, J. Booij, T. Musacchio, S. Klebe, E. Sittig-Wiegand, J. Volkmann, C. Sommer, W.H. Oertel, Dermal phospho-alpha-synuclein deposits confirm REM sleep behaviour disorder as prodromal Parkinson's disease, Acta Neuropathol. 133 (2017) 535–545.
[7] L. Gan, J.A. Johnson, Oxidative damage and the Nrf2-ARE pathway in neurodegenerative diseases, Biochim Biophys. Acta 1842 (2014) 1208–1218.
[8] G. Gardian, L. Yang, C. Cleren, N.Y. Calingasan, P. Klivenyi, M.F. Beal, Neuroprotective effects of phenylbutyrate against MPTP neurotoxicity, Neuromol. Med. 5 (2004) 235–241.
[9] J.D. Haines, O. Herbin, B. de la Hera, O.G. Vidaurre, G.A. Moy, Q. Sun, H.Y. Fung, S. Albrecht, K. Alexandropoulos, D. McCauley, Y.M. Chook, T. Kuhlmann, G. J. Kidd, S. Shacham, P. Casaccia, Nuclear export inhibitors avert progression in preclinical models of inflammatory demyelination, Nat. Neurosci. 18 (2015) 511–520.
[10] I.F. Harrison, W.R. Crum, A.C. Vernon, D.T. Dexter, Neurorestoration induced by the HDAC inhibitor sodium valproate in the lactacystin model of Parkinson's is associated with histone acetylation and up-regulation of neurotrophic factors, Br. J. Pharm. 172 (2015) 4200–4215.
[11] M. Herkenham, M.D. Little, K. Bankiewicz, S.C. Yang, S.P. Markey, J. N. Johannessen, Selective retention of MPP+ within the monoaminergic systems of the primate brain following MPTP administration: an in vivo autoradiographic study, Neuroscience 40 (1991) 133–158.
[12] C.W. Ip, S.K. Beck, J. Volkmann, Lymphocytes reduce nigrostriatal deficits in the 6-hydroxydopamine mouse model of Parkinson's disease, J. Neural Transm. 122 (2015) 1633–1643.
[13] A. Jazwa, A.I. Rojo, N.G. Innamorato, M. Hesse, J. Fernandez-Ruiz, A. Cuadrado, Pharmacological targeting of the transcription factor Nrf2 at the basal ganglia provides disease modifying therapy for experimental parkinsonism, Antioxid. Redox Signal 14 (2011) 2347–2360.
[14] J.A. Johnson, D.A. Johnson, A.D. Kraft, M.J. Calkins, R.J. Jakel, M.R. Vargas, P. C. Chen, The Nrf2-ARE pathway: an indicator and modulator of oxidative stress in neurodegeneration, Ann. N. Y. Acad. Sci. 1147 (2008) 61–69.
[15] N.A. Kaidery, R. Banerjee, L. Yang, N.A. Smirnova, D.M. Hushpulian, K.T. Liby, C. R. Williams, M. Yamamoto, T.W. Kensler, R.R. Ratan, M.B. Sporn, M.F. Beal, I. G. Gazaryan, B. Thomas, Targeting Nrf2-mediated gene transcription by extremely potent synthetic triterpenoids attenuate dopaminergic neurotoxicity in the MPTP mouse model of Parkinson's disease, Antioxid. Redox Signal 18 (2013) 139–157.
[16] L.V. Kalia, A.E. Lang, Parkinson's disease, Lancet 386 (2015) 896–912.
[17] T. Kim, S. Song, Y. Park, S. Kang, H. Seo, HDAC inhibition by valproic acid induces neuroprotection and improvement of PD-like behaviors in LRRK2 R1441G transgenic mice, Exp. Neurobiol. 28 (2019) 504–515.
[18] J.B. Koprich, T.H. Johnston, P. Huot, M.G. Reyes, M. Espinosa, J.M. Brotchie, Progressive neurodegeneration or endogenous compensation in an animal model of Parkinson's disease produced by decreasing doses of alpha-synuclein, PLoS One 6 (2011), e17698.
[19] J.B. Koprich, T.H. Johnston, M.G. Reyes, X. Sun, J.M. Brotchie, Expression of human A53T alpha-synuclein in the rat substantia nigra using a novel AAV1/2 vector produces a rapidly evolving pathology with protein aggregation, dystrophic neurite architecture and nigrostriatal degeneration with potential to model the pathology of Parkinson's disease, Mol. Neurodegener. 5 (2010) 43.
[20] S.E. Lacher, M. Slattery, Gene regulatory effects of disease-associated variation in the NRF2 network, Curr. Opin. Toxicol. 1 (2016) 71–79.
[21] W. Meissner, C. Prunier, D. Guilloteau, S. Chalon, C.E. Gross, E. Bezard, Time-course of nigrostriatal degeneration in a progressive MPTP-lesioned macaque model of Parkinson's disease, Mol. Neurobiol. 28 (2003) 209–218.
[22] B.E. Morrison, N. Majdzadeh, X. Zhang, A. Lyles, R. Bassel-Duby, E.N. Olson, S. R. D'Mello, Neuroprotection by histone deacetylase-related protein, Mol. Cell Biol. 26 (2006) 3550–3564.
[23] T. Musacchio, M. Rebenstorff, F. Fluri, J.M. Brotchie, J. Volkmann, J.B. Koprich, C. W. Ip, Subthalamic nucleus deep brain stimulation is neuroprotective in the A53T alpha-synuclein Parkinson's disease rat model, Ann. Neurol. 81 (2017) 825–836.
[24] K.L. O'Malley, The role of axonopathy in Parkinson's disease, Exp. Neurobiol. 19 (2010) 115–119.
[25] S. Orimo, T. Uchihara, A. Nakamura, F. Mori, A. Kakita, K. Wakabayashi, H. Takahashi, Axonal α-synuclein aggregates herald centripetal degeneration of cardiac sympathetic nerve in Parkinson's disease, Brain 131 (2008) 642–650.
[26] G. Park, J. Tan, G. Garcia, Y. Kang, G. Salvesen, Z. Zhang, Regulation of histone acetylation by autophagy in Parkinson disease, J. Biol. Chem. 291 (2016) 3531–3540.
[27] G. Paxinos, C. Watson. The rat Brain in Stereotaxic Coordinates, Sixth ed.,, Academic Press/Elsevier, Amsterdam; Boston, 2007.
[28] S. Petrillo, T. Schirinzi, G. Di Lazzaro, J. D'Amico, V.L. Colona, E. Bertini, M. Pierantozzi, L. Mari, N.B. Mercuri, F. Piemonte, A. Pisani, Systemic activation of Nrf2 pathway in Parkinson's disease, Mov. Disord. 35 (2020) 180–184.
[29] M.H. Polymeropoulos, C. Lavedan, E. Leroy, S.E. Ide, A. Dehejia, A. Dutra, B. Pike, H. Root, J. Rubenstein, R. Boyer, E.S. Stenroos, S. Chandrasekharappa, A. Athanassiadou, T. Papapetropoulos, W.G. Johnson, A.M. Lazzarini, R. C. Duvoisin, G. Di Iorio, L.I. Golbe, R.L. Nussbaum, Mutation in the alpha-SYnuclein Gene Identified in Families with Parkinson's disease, Science 276 (1997) 2045–2047.
[30] C.P. Ramsey, C.A. Glass, M.B. Montgomery, K.A. Lindl, G.P. Ritson, L.A. Chia, R. L. Hamilton, C.T. Chu, K.L. Jordan-Sciutto, Expression of Nrf2 in neurodegenerative diseases, J. Neuropathol. Exp. Neurol. 66 (2007) 75–85.
[31] G. Sadri-Vakili, B. Bouzou, C.L. Benn, M.O. Kim, P. Chawla, R.P. Overland, K. E. Glajch, E. Xia, Z. Qiu, S.M. Hersch, T.W. Clark, G.J. Yohrling, J.H. Cha, Histones associated with downregulated genes are hypo-acetylated in Huntington's disease models, Hum. Mol. Genet 16 (2007) 1293–1306.
[32] G. Skibinski, V. Hwang, D.M. Ando, A. Daub, A.K. Lee, A. Ravisankar, S. Modan, M. M. Finucane, B.A. Shaby, S. Finkbeiner, Nrf2 mitigates LRRK2- and alpha-synuclein-induced neurodegeneration by modulating proteostasis, Proc. Natl. Acad. Sci. USA 114 (2017) 1165–1170.
[33] C. Song, A. Kanthasamy, V. Anantharam, F. Sun, A.G. Kanthasamy, Environmental neurotoxic pesticide increases histone acetylation to promote apoptosis in dopaminergic neuronal cells: relevance to epigenetic mechanisms of neurodegeneration, Mol. Pharm. 77 (2010) 621–632.
[34] M.G. Spillantini, M.L. Schmidt, V.M. Lee, J.Q. Trojanowski, R. Jakes, M. Goedert, Alpha-synuclein in Lewy bodies, Nature 388 (1997) 839–840.

[35] N.P. Visanji, J.M. Brotchie, L.V. Kalia, J.B. Koprich, A. Tandon, J.C. Watts, A. E. Lang, alpha-Synuclein-based animal models of parkinson's disease: challenges and opportunities in a new era, Trends Neurosci. 39 (2016) 750–762.

[36] M. von Otter, P. Bergström, A. Quattrone, E.V. De Marco, G. Annesi, P. Söderkvist, S.B. Wettinger, M. Drozdzik, M. Bialecka, H. Nissbrandt, C. Klein, M. Nilsson, O. Hammarsten, S. Nilsson, H. Zetterberg, Genetic associations of Nrf2-encoding NFE2L2 variants with Parkinson's disease - a multicenter study, BMC Med. Genet. 15 (2014) 131.

[37] J.C. Ximenes, K.R. Neves, L.K. Leal, M.R. do Carmo, G.A. Brito, G. Naffah-Mazzacoratti Mda, E.A. Cavalheiro, G.S. Viana, Valproic ACid Neuroprotection in the 6-OHDA model of Parkinson's disease is possibly related to its anti-inflammatory and HDAC inhibitory properties, J. Neurodegener. Dis. 2015 (2015), 313702.